Quantum Dot Self-Assembly Driven by a Surfactant-Induced Morphological Instability

Ryan B. Lewis,[1,*] Pierre Corfdir,[1] Hong Li,[1,2] Jesús Herranz,[1] Carsten Pfüller,[1] Oliver Brandt,[1] and Lutz Geelhaar[1]
[1]Paul-Drude-Institut für Festkörperelektronik, Hausvogteiplatz 5-7, 10117 Berlin, Germany
[2]Institut für Physik und IRIS Adlershof, Humboldt-Universität zu Berlin, Zum Großen Windkanal 6, 12489 Berlin, Germany
(Received 27 February 2017; published 24 August 2017)

In strained heteroepitaxy, two-dimensional layers can exhibit a critical thickness at which three-dimensional islands self-assemble, relieving misfit strain at the cost of an increased surface area. Here we show that such a morphological phase transition can be induced on demand using surfactants. We explore Bi as a surfactant in the growth of InAs on GaAs(110), and find that the presence of surface Bi induces Stranski-Krastanov growth of 3D islands, while growth without Bi always favors 2D layer formation. Exposing a static two monolayer thick InAs layer to Bi rapidly transforms the layer into 3D islands. Density functional theory calculations reveal that Bi as well as Sb reduce the energetic cost of 3D island formation by modifying surface energies. These 3D nanostructures behave as optically active quantum dots. This work illustrates how surfactants can enable quantum dot self-assembly where it otherwise would not occur.

DOI: 10.1103/PhysRevLett.119.086101

Three-dimensional (3D) islands that act as quantum dots (QDs) are typically synthesized by a self-assembly process known as Stranski-Krastanov (SK) growth, one of the three fundamental modes of epitaxy [1,2]. In general, the preferred growth mode of a system is determined by energetic considerations (surface, interface, strain), which are fixed by the choice of adsorbate and substrate. To some extent these thermodynamic constraints can be overcome kinetically, either by adjusting deposition conditions [3] or by changing the surface chemistry using surface segregating elements [4–8], allowing 3D island formation to be kinetically suppressed in favor of two-dimensional (2D) Frank–van der Merwe (FM) growth. However, control over the energetically preferred growth mode, as well as inducing 3D island formation when 2D growth is favored, has remained elusive. And as a result, QD synthesis has been restricted in terms of materials and substrate orientations.

The (In,Ga)As/GaAs(100) system is the most extensively explored SK growth system, demonstrating (In,Ga)As QDs suitable for quantum optics applications requiring single photon emission [9,10] and emission of entangled photon pairs [11,12]. While (In,Ga)As favors SK growth for a wide range of compositions and deposition conditions on GaAs(100), on other low-index GaAs surfaces such as (110) and (111), growth occurs via a 2D FM mode and misfit strain relaxes plastically [13–16]. Because of the low surface energy of GaAs(110), {110} facets are often present in self-assembled GaAs nanostructures such as nanowires and the growth of QDs on these structures is of interest for high brightness single photon sources [17,18].

Here we show that surfactants can provoke morphological phase transitions in strained layers, inducing the formation of 3D islands "on demand." We investigate Bi as a surfactant in the growth of InAs on GaAs(110) by molecular beam epitaxy (MBE). The presence of surface Bi is found to alter the fundamental growth mode of InAs, inducing 3D island formation by the SK mechanism. Furthermore, surface Bi can provoke a morphological phase transition in static 2D InAs layers, inducing a rapid rearrangement of the 2D layer into 3D islands. Density functional theory (DFT) calculations reveal that surface Bi, and also Sb, reduce the energetic cost of 3D island formation by altering the surface energy of the GaAs and InAs surfaces. Photoluminescence (PL) spectroscopy on these novel nanostructures demonstrates that they behave as optically active QDs. This work illustrates how modifying surface energies with surfactants can allow for unprecedented control over nanostructure self-assembly.

Samples were grown by MBE on 2" GaAs(110) wafers. Fluxes were provided by effusion cells for Ga, In, and Bi, and a valved cracker for As_2. A substrate temperature of 420 °C and an As flux of 1.1 nm/s GaAs equivalent growth rate were maintained for the entire deposition process. GaAs buffer layers (50–150 nm thick) and capping layers (50 nm thick) were deposited at 0.28 nm/s. For experiments exploring concurrent In and Bi deposition, the Bi flux was initiated 20 s before the In flux to produce a stable Bi coverage. The Bi beam equivalent pressure (BEP) was 2×10^{-6} mbar (about 0.4 ML/s) and the In flux was 0.14 ML/s. In further experiments, Bi was deposited subsequent to InAs, and in this case the Bi flux was maintained for 30 s before cooling the sample at 2 °C/s while maintaining the As_2 flux, until the substrate was below 350 °C. Samples for photoluminescence (PL) studies were capped with 50 nm of GaAs.

Density functional theory calculations were performed with the Vienna *ab initio* simulation package (VASP) [19,20]. The *d* electrons for Ga, In, Sb, and Bi were considered as valence states, and the (110) surfaces were modeled with a slab consisting of nine atomic layers and a

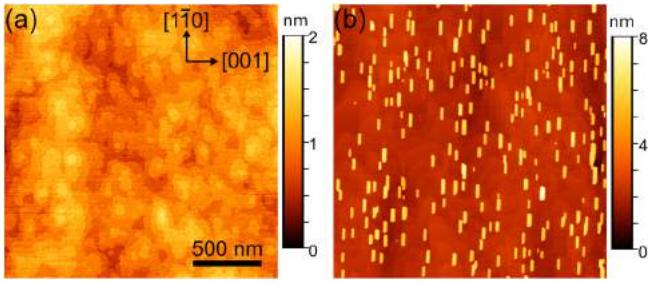

FIG. 1. Surface topographs after deposition of 2.1 ML of InAs on GaAs(110) (a) in the absence of Bi and (b) with a Bi flux. In the absence of Bi the surface is atomically smooth, while growth with the Bi flux results in 3D islands. The scale bar and crystallographic directions shown in (a) also apply to (b).

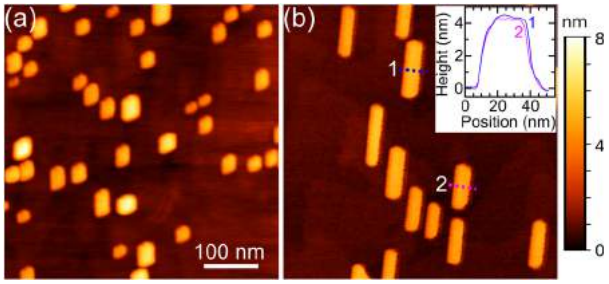

FIG. 2. Comparison of InAs 3D islands formed by two approaches: (a) exposing a static 2.1 ML 2D InAs layer to Bi and (b) depositing 2.1 MLs of InAs while simultaneously depositing Bi to induce SK growth. The height and density of the 3D islands in (a) are 4.6 ± 1.3 nm and about 1.7×10^{10} cm^{-2}, respectively. The scale is the same for both images and the [1$\bar{1}$0] direction is approximately upward. The total volume of the 3D islands in (a) and (b) corresponds to approximately 1.9 and 1.7 ML of 2D growth, respectively, assuming the islands are composed of coherent InAs. The inset shows line scans across two islands.

vacuum of 20 Å. Pseudohydrogen atoms with partial charge of 0.75 (1.25) were used to passivate the dangling bonds of the bottom surface As (Ga) atoms [21]. The local-density approximation (LDA) was chosen for the exchange-correlation functional. The calculated surface energies were 50.6 and 40.2 meV/Å^2 for GaAs (110) and InAs (110), respectively, in good agreement with other calculations [22].

Magneto-PL experiments were performed at 4.2 K in a confocal setup operating in Faraday geometry (magnetic field parallel to the [110] direction) with magnetic field strength between 0 and 8 T. The samples were excited using a Ti:sapphire laser emitting at 790 nm, and the laser spot diameter and power at the surface of the samples were 1 μm and 10 μW, respectively. The PL signal was dispersed using a monochromator and detected with a charge-coupled device camera.

Figure 1 shows atomic force microscopy (AFM) topographs after deposition of 2.1 monolayers (MLs) of InAs on GaAs(110), without and with the presence of a Bi flux during the InAs deposition. We note that 2.1 MLs on GaAs(110) corresponds to 1.5 MLs on GaAs(100). In the absence of Bi [Fig. 1(a)], InAs forms a 2D layer with atomic terraces on the surface. The addition of a Bi flux [Fig. 1(b)] results in a drastically different surface morphology, showing an array of 3D islands with a density of 6×10^9 cm^{-2} and an average height of 4.3 nm (standard deviation 0.5 nm). The presence of 3D islands is in striking contrast to the expectation that InAs deposition on GaAs(110) always proceeds by a 2D FM mode. However, we note that the growth of InAs 3D islands has been demonstrated on GaAs(110) substrates covered by thin (In,Ga)As [23,24] and AlAs layers [25]. The islands in Fig. 1(b) are elongated in the [1$\bar{1}$0] direction, possibly a result of the elastic anisotropy or the higher adatom diffusion along [1$\bar{1}$0]. AFM line scans indicate flat (110) tops and sidewalls inclined by about 35°, consistent with {111} facets [Fig. 2(b)]. During the growth of this sample, the reflection high energy electron diffraction (RHEED) pattern showed a streaky-to-spotty (2D-to-3D) transition at a thickness of about 1.9 ML. The observation of a critical thickness for 3D island nucleation is consistent with SK growth. Conversely, increasing the InAs thicknesses to 4.2 MLs in the absence of Bi does not result in 3D nanostructure formation; see the Supplemental Material [26].

Energy-dispersive x-ray spectroscopy investigation of samples grown with Bi BEPs higher than 2×10^{-6} mbar only indicated the presence of Bi in the InAs 3D islands above about 1×10^{-5} mbar. Bi is not expected to form a compound with InAs at the high As/In flux ratios used in this study [31], and the incorporation of some Bi is not expected to degrade the optoelectronic properties of InAs. In fact, using surfactant Bi during InAs QD growth on GaAs(100) has been shown to greatly improve QD photoluminescence [32].

The above results show that the presence of surface Bi can alter the fundamental growth mode of InAs on GaAs(110) from 2D to 3D. In the absence of Bi, 3D islands never form because the critical thickness for their formation is larger than the critical thickness for plastic relaxation (previously reported to be 2–3 MLs) [15]. With the presence of surface Bi, the situation is reversed. To further explore the effect of surface Bi on the morphological stability of InAs, we expose a 2.1 ML thick 2D InAs layer grown without Bi [Fig. 1(a)] to a subsequent Bi flux for 30 s. Figure 2(a) shows the resulting surface topography, which is compared to 3D islands grown at the same conditions but with simultaneous InAs and Bi deposition [Fig. 2(b), same sample as in Fig. 1(b)]. Remarkably, exposing the 2D InAs layer to Bi results in a rearrangement of the InAs into 3D islands. Compared to the sample grown with codeposition of Bi and InAs [Fig. 2(b)], the island density is about 3 times higher and the dots are more symmetric, suggesting that island nucleation occurs more rapidly. The initiation of the Bi exposure produces an

abrupt transition of the RHEED pattern from 2D streaks to 3D spots. Therefore, surface Bi can provoke a morphological phase transition in a static InAs layer, indicating that the effect of surface Bi goes beyond modifying adatom kinetics during InAs growth. In the absence of Bi, the 2.1 ML InAs thickness is below the critical thicknesses for both 3D island formation and plastic relaxation, but in the presence of Bi the layer is thicker than the critical thickness for 3D island formation. Therefore, the morphological stability of the layer can be controlled externally through the Bi coverage, allowing a morphological phase transition to be induced on-demand. This unprecedented external control opens up new possibilities for 3D nanostructure self-assembly.

Surface segregating elements such as Sb, Te, and Bi, have been previously investigated in the growth of (In,Ga)As, although only on the (100) surface of GaAs. In contrast to the present findings for Bi, Sb, and Te have been shown to inhibit 3D growth, by dramatically reducing adatom diffusion [6,33]. While Bi has been found to actually increase adatom diffusion during 2D growth [34], the surfactant effect of Bi in III-V epitaxy has been only sparsely explored [32,34–38].

The formation of 3D islands during epitaxy has been investigated theoretically in terms of Asaro-Tiller-Grinfeld (ATG) linear instability theory [39,40], as well as nucleation theory [41]. The roughening of a 2D layer is driven by strain relaxation but inhibited by surface energy. To elucidate the effect of surface Bi on the surface energy, we carried out DFT calculations. As Sb is a popular surfactant, we performed calculations for this element as well. We consider various surface configurations and compare the surface formation energies relative to the energy of the relaxed bulk-truncated 1×1 GaAs(110) surface. The relative surface formation energy is defined as

$$\Delta\gamma = \left[E_{\text{surf}} - E_{\text{ref}} - \sum_i n_i \mu_i\right]/A, \qquad (1)$$

where E_{surf} and E_{ref} are the total energies calculated for the surface structure and the reference 1×1 GaAs(110) structure, n_i and μ_i are the excess number of atoms (compared to the reference structure) and the chemical potential of element i, respectively, and A is the surface area. The chemical potentials of GaAs, InAs, Sb, and Bi were deduced from the calculated total energies for their bulk structures. The relative surface energy includes contributions from the strain energy, as well as energy changes due to the surface and interfaces. In the absence of InAs, we find that the most stable configuration for GaAs(110) is a single Bi adlayer covering the 1×1 GaAs surface. Similarly, for InAs on 1×1 GaAs(110) the 1×1 surface structure is found to be the most stable; see the Supplemental Material [26]. We note that experimentally we observe only a 1×1 RHEED pattern and this is consistent with previous observations of InAs deposition on GaAs(110) [15].

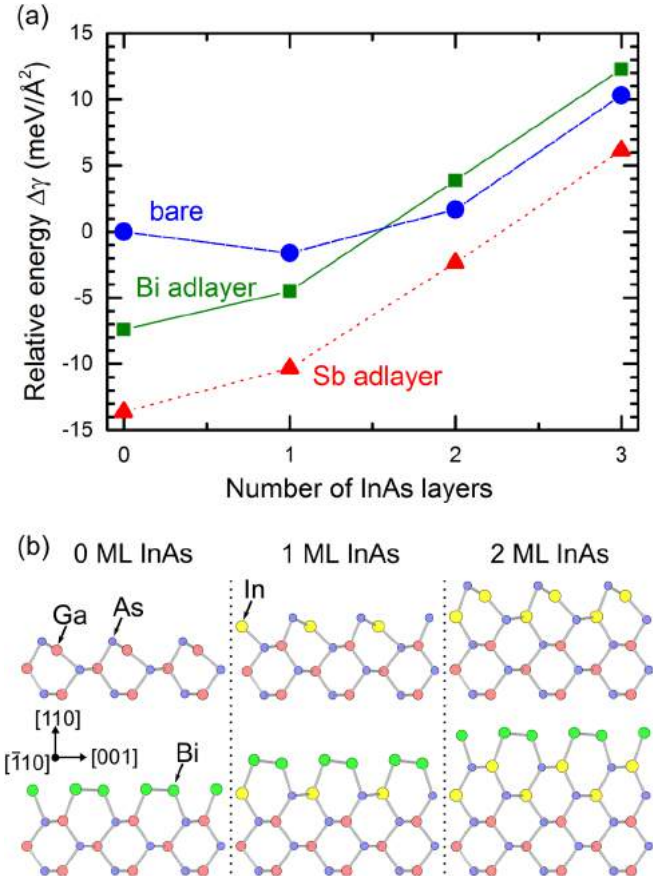

FIG. 3. Relative surface energy and structure of InAs/GaAs(110) for varying InAs coverage with and without a Bi adlayer. (a) Relative surface formation energies calculated by DFT for the Bi and Sb terminated and bare surfaces assuming the 1×1 epitaxial continued layer structure. The in-plane lattice parameter is fixed to that of bulk GaAs. (b) Surface structures for 0–2 ML InAs coverage without (upper row) and with (lower row) the Bi adlayer.

Therefore, for calculations involving InAs epilayers on GaAs(110) we consider only 1×1 surfaces and a single Bi adlayer. We note that growth of InAs on top of a Bi monolayer is highly energetically unfavorable (see the Supplemental Material [26]). Therefore, during InAs growth the Bi layer is expected to remain on the surface.

Figure 3(a) displays the relative surface energy as a function of the InAs thickness on GaAs(110) with and without Bi and Sb adlayer coverage. In the absence of Bi or Sb, $\Delta\gamma$ is negative for an InAs coverage of 1 ML due to the lower InAs surface energy, but positive for higher coverages as a result of strain. Therefore, it is energetically preferable for InAs to wet the GaAs(110) surface. However, beyond 1 ML coverage, the layer is metastable. Since $\Delta\gamma$ increases with increasing InAs coverage, eventually a critical thickness is reached where the layer relaxes plastically (reported to be 2–3 ML [15]). With the addition of a Bi adlayer, the situation is strikingly different. In this case, the Bi terminated GaAs(110) surface (0 ML InAs) shows a large negative $\Delta\gamma$ of -7.4 meV/Å^2. Thus, Bi behaves as a

surfactant on GaAs, reducing the surface energy. With increasing InAs wetting layer thickness $\Delta\gamma$ increases monotonically, due to the increasing strain energy. In contrast to the case without Bi, the lowest energy surface does not contain an InAs wetting layer. The situation is qualitatively similar for Sb. For InAs coverages of 2 and 3 ML, the presence of the Bi adlayer increases $\Delta\gamma$. This can be understood by considering the surface structures presented in Fig. 3(b), for 0–2 ML InAs coverage with and without Bi, where stronger bond relaxation and re-hybridization are found to occur on the bare GaAs and InAs surfaces. As Bi suppresses the distortion of the InAs lattice, it is expected that the InAs strain energy is higher in the presence of Bi. This could explain why the relative surface energy is larger with Bi than without at higher InAs thicknesses.

The DFT results indicate that the Bi adlayer reduces the relative surface energies of bulk GaAs(110) and InAs(110) (see the Supplemental Material for bulk InAs) [26]. Furthermore, surface Bi reduces the thermodynamic driving force for InAs wetting on GaAs(110), as the lowest energy state is Bi-terminated GaAs(110). In other words, 2D InAs layers under the Bi adlayer always have an energy greater than Bi-terminated GaAs(110) plus bulk InAs, suggesting that even Volmer–Weber growth may be possible on the Bi-terminated surface. Finally, Bi inhibits bond relaxation at the InAs surface, increasing the InAs strain energy. All of these effects will favor 3D island formation compared to the case without Bi. For SK growth, the energy barrier for 3D island formation is believed to control the critical thickness for islanding [2,41]. This energy barrier is related to the surface energy as well as strain energy. Therefore, the DFT results are consistent with Bi reducing the energy barrier and hence the critical thickness for 3D island formation, which RHEED measurements indicate is nonzero. Such a surfactant-induced lowering of the energy barrier for 3D island formation has been predicted theoretically [42]. Finally, the DFT results suggest a similar effect for Sb, implying a general nature for the phenomena demonstrated here with Bi.

To investigate whether Bi surfactant-induced 3D islands can behave as optically active QDs, a sample with about 1.5 ML of InAs grown with In and Bi codeposition and then capped with GaAs was investigated by PL. The insets of Fig. 4(b) presents AFM topographs from an uncapped sample with a similar InAs nominal thickness of 1.7 MLs (below the 2D-3D RHEED transition), showing small 3D islands of about 10 nm in diameter on the surface at a low density of about 10^8 cm^{-2}. The capped sample is expected to exhibit similar islands, and we speculate that with further InAs deposition these small islands enlarge into the islands presented in Figs. 1 and 2. A PL spectrum taken on the capped sample is displayed in Fig. 4(a), where a set of transitions with linewidths of about 0.36 meV (resolution limited) is observed between 1.29 and 1.34 eV. For samples grown without Bi such transitions are not detected,

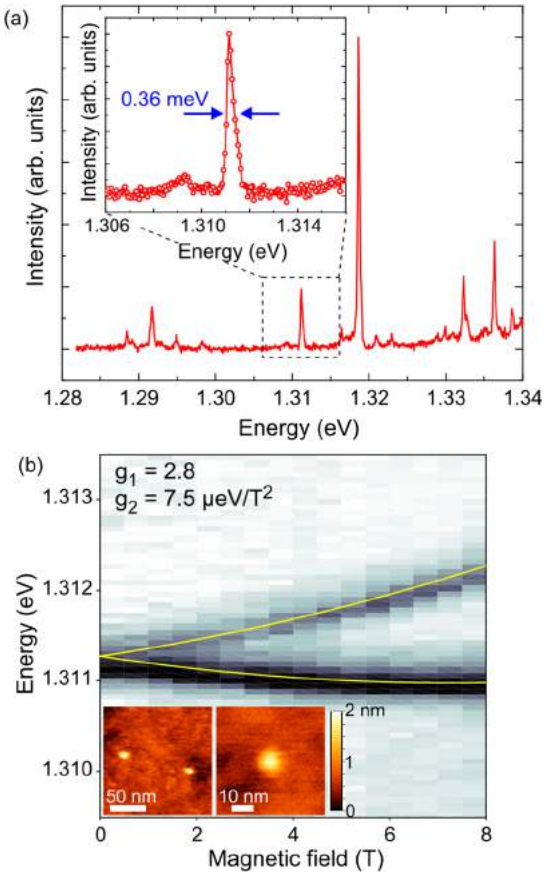

FIG. 4. (a) Photoluminescence spectrum from a few InAs QDs on GaAs(110) displaying a series of narrow transitions. The inset shows emission from a single InAs QD with full width at half maximum 0.36 meV (resolution limit). (b) Magneto-PL intensity map from the QD transition shown in the inset in (a). The quadratic fits to the QD emission energy as a function of magnetic field account for Zeeman and diamagnetic effects, yielding an exciton g factor $g_1 = 2.8$ and a diamagnetic shift $g_2 = 7.5\,\mu\text{eV}/\text{T}^2$. The insets show exemplary AFM images of small QDs from an uncapped sample grown with 1.7 ML InAs.

suggesting that they originate from the surfactant-induced 3D islands. An enlarged PL spectrum of a typical transition is shown in the inset. With increasing excitation power, the intensity of this line increases linearly (see the Supplemental Material) [26], showing that it is related to the recombination of a neutral exciton. The emission energy range in Fig. 4(a) corresponds to the one usually observed for excitons strongly confined in SK InAs QDs grown on GaAs(100). To obtain quantitative information on the size of the 3D islands giving rise to these transitions, we followed their energy in a magnetic field. Figure 4(b) shows the evolution between 0 and 8 T of the transition shown in the inset of Fig. 4(a). This line splits into two transitions, whose energies follow a parabolic dependence with increasing magnetic field. A parabolic fit to these emission energies [43] yields an exciton g factor $g_1 = 2.8$ and a diamagnetic shift $g_2 = 7.5\,\mu\text{eV}/\text{T}^2$. For neutral

excitons, g_2 is proportional to the electron-hole coherence length (L_{eh}) in the plane perpendicular to the magnetic field [43]. Measuring g_2 for a total of 14 transitions, we obtain an average in-plane L_{eh} of 5.4 ± 1.2 nm. This value, which corresponds to the radius of the 3D islands giving rise to light emission in the 1.3 to 1.4 eV range, is consistent with the size of the islands shown in the insets of Fig. 4(b). We therefore attribute the observed PL emission to these objects. These results demonstrate that the surfactant Bi can enable the growth of optically active QDs on a surface where QD growth is otherwise inhibited.

In conclusion, morphological phase transitions in strained films can be induced by externally modifying surface energies with surfactants. We have used this approach to synthesize optically active quantum dots where they would otherwise not form. This unprecedented external control over the self-assembly of 3D nanostructures paves the way to realizing quantum dots with new materials and on new substrates, and provides an experimental framework to test theories of strained heteroepitaxy.

R. B. L. acknowledges funding from the Alexander von Humboldt Foundation. P. C. acknowledges funding from the Fonds National Suisse de la Recherche Scientifique through Project No. 161032. The authors are grateful to M. Höricke and C. Stemmler for MBE maintenance, M. Ramsteiner and G. Paris for Magneto-PL help, and V. M. Kaganer for a critical reading of the manuscript.

*lewis@pdi-berlin.de

[1] W. Seifert, N. Carlsson, M. Miller, M.-E. Pistol, L. Samuelson, and L. R. Wallenberg, Prog. Cryst. Growth Charact. Mater. **33**, 423 (1996).
[2] J. Stangl, V. Holý, and G. Bauer, Rev. Mod. Phys. **76**, 725 (2004).
[3] C. W. Snyder, J. F. Mansfield, and B. G. Orr, Phys. Rev. B **46**, 9551 (1992).
[4] M. Copel, M. C. Reuter, E. Kaxiras, and R. M. Tromp, Phys. Rev. Lett. **63**, 632 (1989).
[5] M. Copel, M. C. Reuter, M. Horn von Hoegen, and R. M. Tromp, Phys. Rev. B **42**, 11682 (1990).
[6] N. Grandjean, J. Massies, and V. H. Etgens, Phys. Rev. Lett. **69**, 796 (1992).
[7] E. Tournié and K. H. Ploog, Thin Solid Films **231**, 43 (1993).
[8] B. Voigtlander, A. Zinner, T. Weber, and H. P. Bonzel, Phys. Rev. B **51**, 7583 (1995).
[9] C. Santori, M. Pelton, G. Solomon, Y. Dale, and Y. Yamamoto, Phys. Rev. Lett. **86**, 1502 (2001).
[10] Z. Yuan, B. E. Kardynal, R. M. Stevenson, A. J. Shields, C. J. Lobo, K. Cooper, N. S. Beattie, D. A. Ritchie, and M. Pepper, Science **295**, 102 (2002).
[11] R. M. Stevenson, R. J. Young, P. Atkinson, K. Cooper, D. A. Ritchie, and A. J. Shields, Nature (London) **439**, 179 (2006).
[12] C. L. Salter, R. M. Stevenson, I. Farrer, C. A. Nicoll, D. A. Ritchie, and A. J. Shields, Nature (London) **465**, 594 (2010).
[13] X. Zhang and D. W. Pashley, J. Mater. Sci. Mater. Electron. **7**, 361 (1996).
[14] J. G. Belk, J. L. Sudijono, X. M. Zhang, J. H. Neave, T. S. Jones, and B. A. Joyce, Phys. Rev. Lett. **78**, 475 (1997).
[15] B. A. Joyce, J. L. Sudijono, J. G. Belk, H. Yamaguchi, X. M. Zhang, H. T. Dobbs, A. Zangwill, D. D. Vvedensky, and T. S. Jones, Jpn. J. Appl. Phys. **36**, 4111 (1997).
[16] B. A. Joyce and D. D. Vvedensky, Mater. Sci. Eng. R **46**, 127 (2004).
[17] E. Uccelli, J. Arbiol, J. R. Morante, and A. Fontcuberta i Morral, ACS Nano **4**, 5985 (2010).
[18] M. Heiss, Y. Fontana, A. Gustafsson, G. Wüst, C. Magen, D. D. O'Regan, J. W. Luo, B. Ketterer, S. Conesa-Boj, A. V. Kuhlmann, J. Houel, E. Russo-Averchi, J. R. Morante, M. Cantoni, N. Marzari, J. Arbiol, A. Zunger, R. J. Warburton, and A. Fontcuberta i Morral, Nat. Mater. **12**, 439 (2013).
[19] G. Kresse and J. Furthmüller, Phys. Rev. B **54**, 11169 (1996).
[20] G. Kresse and D. Joubert, Phys. Rev. B **59**, 1758 (1999).
[21] J. Li and L.-W. Wang, Phys. Rev. B **72**, 125325 (2005).
[22] T. Hammerschmidt, P. Kratzer, and M. Scheffler, Phys. Rev. B **77**, 235303 (2008).
[23] M. Blumin, H. E. Ruda, I. G. Savelyev, A. Shik, and H. Wang, J. Appl. Phys. **99**, 093518 (2006).
[24] A. Aierken, T. Hakkarainen, M. Sopanen, J. Riikonen, J. Sormunen, M. Mattila, and H. Lipsanen, Appl. Surf. Sci. **254**, 2072 (2008).
[25] D. Wasserman, S. A. Lyon, M. Hadjipanayi, A. Maciel, and J. F. Ryan, Appl. Phys. Lett. **83**, 5050 (2003).
[26] See Supplemental Material http://link.aps.org/supplemental/10.1103/PhysRevLett.119.086101 for an AFM image of a 4.2 ML thick InAs layer grown without Bi surfactant, additional surface energy calculations, and the excitation power dependence of QD photoluminescence, which includes Refs. [27–30].
[27] J. Neugebauer and M. Scheffler, Phys. Rev. B **46**, 16067 (1992).
[28] H. J. Monkhorst and J. D. Pack, Phys. Rev. B **13**, 5188 (1976).
[29] D. N. McIlroy, D. Heskett, D. M. Swanston, A. B. McLean, R. Ludeke, H. Munekata, M. Prietsch, and N. J. DiNardo, Phys. Rev. B **47**, 3751 (1993).
[30] M. G. Betti, V. Corradini, U. del Pennino, V. De Renzi, P. Fantini, and C. Mariani, Phys. Rev. B **58**, R4231 (1998).
[31] P. T. Webster, N. A. Riordan, C. Gogineni, S. Liu, J. Lu, X.-H. Zhao, D. J. Smith, Y.-H. Zhang, and S. R. Johnson, J. Vac. Sci. Technol. B **32**, 02C120 (2014).
[32] H. Okamoto, T. Tawara, H. Gotoh, H. Kamada, and T. Sogawa, Jpn. J. Appl. Phys. **49**, 06GJ01 (2010).
[33] J.-C. Harmand, L. H. Li, G. Patriarche, and L. Travers, Appl. Phys. Lett. **84**, 3981 (2004).
[34] S. Tixier, M. Adamcyk, E. C. Young, J. H. Schmid, and T. Tiedje, J. Cryst. Growth **251**, 449 (2003).
[35] M. R. Pillai, S.-S. Kim, S. T. Ho, and S. A. Barnett, J. Vac. Sci. Technol. B **18**, 1232 (2000).
[36] E. C. Young, S. Tixier, and T. Tiedje, J. Cryst. Growth **279**, 316 (2005).

[37] B. N. Zvonkov, I. A. Karpovich, N. V Baidus, D. O. Filatov, S. V Morozov, and Y. Y. Gushina, Nanotechnology **11**, 221 (2000).
[38] D. Fan, Z. Zeng, V. G. Dorogan, Y. Hirono, C. Li, Y. I. Mazur, S. Q. Yu, S. R. Johnson, Z. M. Wang, and G. J. Salamo, J. Mater. Sci. Mater. Electron. **24**, 1635 (2013).
[39] R. Asaro and W. Tiller, Metall. Trans. **3**, 1789 (1972).
[40] M. A. Grinfel'd, Sov. Phys. Dokl. **31**, 831 (1986).
[41] J. Tersoff and F. K. LeGoues, Phys. Rev. Lett. **72**, 3570 (1994).
[42] A. A. Tonkikh and P. Werner, Phys. Status Solidi (a) **250**, 1795 (2013).
[43] B. Van Hattem, P. Corfdir, P. Brereton, P. Pearce, A. M. Graham, M. J. Stanley, M. Hugues, M. Hopkinson, and R. T. Phillips, Phys. Rev. B **87**, 205308 (2013).